Published in final edited form as:
J Bone Miner Res. 2011 November ; 26(11): 2622–2633. doi:10.1002/jbmr.502.

The Critical Role of the Epidermal Growth Factor Receptor in Endochondral Ossification

Xianrong Zhang[1], **Valerie A. Siclari**[1], **Shenghui Lan**[1,2], **Ji Zhu**[1], **Eiki Koyama**[3], **Holly L. Dupuis**[4], **Motomi Enomoto-Iwamoto**[3], **Frank Beier**[4], and **Ling Qin**[1,*]

[1]Department of Orthopaedic Surgery, School of Medicine, University of Pennsylvania, Philadelphia, Pennsylvania, USA

[2]Department of Orthopaedics, Union Hospital, Tongji Medical College, Huazhong University of Science and Technology, Hubei Province, People's Republic of China

[3]Department of Surgery, The Children's Hospital of Philadelphia, Philadelphia, USA

[4]Department of Physiology and Pharmacology, Schulich School of Medicine and Dentistry, University of Western Ontario, London, ON, Canada

Abstract

Loss of epidermal growth factor receptor (EGFR) activity in mice alters growth plate development, impairs endochondral ossification, and retards growth. However, the detailed mechanism by which EGFR regulates endochondral bone formation is unknown. Here, we show that administration of an EGFR-specific small molecule inhibitor, gefitinib, into 1-month-old rats for 7 days produced profound defects in long bone growth plate cartilage characterized by epiphyseal growth plate thickening and massive accumulation of hypertrophic chondrocytes. Immunostaining demonstrated that growth plate chondrocytes express EGFR but endothelial cells and osteoclasts show little to no expression. Gefitinib did not alter chondrocyte proliferation or differentiation and vascular invasion into the hypertrophic cartilage. However, osteoclast recruitment and differentiation at the chondro-osseous junction was attenuated due to decreased RANKL expression in the growth plate. Moreover, gefitinib treatment inhibited the expression of matrix metalloproteinases (MMP9, 13, and 14), increased the amount of collagen fibrils, and decreased degraded extracellular matrix products in the growth plate. In vitro, the EGFR ligand TGFα strongly stimulated RANKL, MMP9 and MMP13 expression and suppressed OPG expression in primary chondrocytes. In addition, a mouse model of cartilage-specific EGFR inactivation exhibited a similar phenotype of hypertrophic cartilage enlargement. Together, our data demonstrate that EGFR signaling supports osteoclastogenesis at the chondro-osseous junction and promotes chondrogenic expression of MMPs in the growth plate. Therefore, we conclude that EGFR signaling plays an essential role in the remodeling of growth plate cartilage extracellular matrix into bone during endochondral ossification.

[*]Corresponding author: Ling Qin, Department of Orthopaedic Surgery, University of Pennsylvania, 424D Stemmler Hall, 36th Street and Hamilton Walk, Philadelphia, PA 19104, Tel: 215-8986697; Fax: 215-5732133; qinling@mail.med.upenn.edu .
Xianrong Zhang: xianrong@mail.med.upenn.edu
Valerie Siclari: vsiclari@mail.med.upenn.edu
Shenghui Lan: shenghuilan@gmail.edu
Ji Zhu: zhuji@mail.med.upenn.edu
Eiki Koyama: koyamae@email.chop.edu
Holly Dupuis: hkipp@uwo.ca
Motomi Enomoto-Iwamoto: IwamotoM1@email.chop.edu
Frank Beier: fbeier@uwo.ca
Ling Qin: qinling@mail.med.upenn.edu

Conflicts of Interest

None of the authors have a conflict of interest.

Keywords

EGFR; endochondral ossification; growth plate; chondrocytes; MMP

Introduction

The majority of the mammalian skeleton, except for most of the craniofacial skeleton, forms through the process of endochondral ossification, in which a cartilage template is replaced by bone. In long bones, this process occurs at the primary and secondary ossification centers separated by the growth plate. The growth plate consists of a distinct polarized layer of chondrocytes. To achieve longitudinal growth, growth plate chondrocytes go through several stages including proliferation, differentiation, hypertrophy, mineralization, and apoptosis. At the chondro-osseous junction (COJ), the invasion of hypertrophic cartilage by blood vessels, osteoclasts and osteoblast precursor cells, together with terminally differentiated hypertrophic chondrocytes, leads to degradation and remodeling of the hypertrophic cartilage extracellular matrix (ECM) into trabecular bone.

Endochondral ossification is tightly controlled by circulating systemic hormones and locally produced signaling factors. These include Indian hedgehog (Ihh), parathyroid hormone (PTH), parathyroid hormone-related protein (PTHrP) and their receptor PTH1R, fibroblast growth factor (FGF)-18 and its receptor FGFR3, vascular endothelial growth factor (VEGF), connective tissue growth factor (CTGF), bone morphogenetic proteins (BMPs), and Wnt proteins. In addition, the transcription factors Sox9 and Runx2/Cbfa1 play major roles in growth plate chondrocyte proliferation and differentiation (reviewed in (1,2)).

The epidermal growth factor receptor (EGFR) belongs to a tyrosine kinase receptor family that also contains ErbB2, ErbB3 and ErbB4. Its ligands include EGF, amphiregulin, and TGFα, which only bind to EGFR, and heparin binding EGF (HB-EGF), betacellulin, and epiregulin, which bind to both EGFR and ErbB4. Upon ligand binding, EGFR either homodimerizes or heterodimerizes with other ErbBs. The dimerized receptors then undergo auto- or trans-phosphorylation on tyrosine residues in the intracellular domain, thus activating several important intracellular signal transduction pathways including Ras-Raf-MAP-kinase and PI-3-kinase-Akt. ErbB2 is the preferred partner for EGFR and the signals mediated by EGFR/ErbB2 are thought to account for most of EGFR's biological activities. EGFR signaling modulates a variety of cell functions such as proliferation, survival, adhesion, migration and differentiation (reviewed in (3)).

Egfr null mice usually die at midgestation, birth or within 20 postnatal days, depending on genetic background, due to severe developmental abnormalities in placental, neural, and epithelial tissues (4-6). A few surviving *Egfr* null pups displayed craniofacial alterations and cleft palates (7). They also had delayed primary endochondral ossification, an enlarged hypertrophic zone in the growth plate, and impaired trabecular bone formation during embryonic development (8). Similarly, mice expressing humanized EGFR (by replacement of the endogenous mouse *Egfr* gene with human EGFR cDNA) exhibited low EGFR activity in the skeleton and had a greatly enlarged hypertrophic chondrocyte zone in the growth plate (9). Overexpression of herstatin, a soluble ErbB2 receptor that acts in a dominant negative fashion to inhibit EGFR signaling, under the limb-specific Prx1 promoter in mice resulted in shortened limbs and an expanded hypertrophic zone (10). In contrast, mice ubiquitously overexpressing the EGFR ligand betacellulin had a smaller hypertrophic zone regardless of age and sex (11). In another transgenic mouse model where human EGF was ubiquitously expressed under the β-actin promoter, the proximal tibial growth plate retained columns of prehypertrophic chondrocytes which was not seen in the control at 6 months of age (12).

Taken together, this data clearly indicate that EGFR signaling plays an important role in long bone development and endochondral ossification but the underlying mechanism is largely unkown.

Gefitinib is a FDA-approved small molecule EGFR inhibitor that blocks EGFR's activity by competing with ATP binding to the receptor's kinase pocket (13). In this study, we treated young growing rats with gefitinib to investigate the effects of blocking EGFR activity on endochondral ossification. Using histological analyses, immunohistochemistry, quantitative measurement of gene and protein expression, and primary chondrocyte cultures, we demonstrate that EGFR signaling plays an essential role in the remodeling of growth plate cartilage ECM into bone during endochondral ossification.

Materials and Methods

Animals

One-month-old male Sprague-Dawley rats (Taconic) were administered with either vehicle (0.5% methyl cellulose) or gefitinib (LC Laboratories, 100 mg/kg/day) daily by oral gavage for 7 days. There was no significant body weight loss after treatment. After euthanization, blood was collected by cardiac puncture to measure serum calcium ion concentration (Calcium Reagent Set, Pointe Scientific). Femurs and tibiae were harvested and processed for growth plate tissue, histological analyses, microCT, and immunohistochemisty.

Egfr$^{f/f}$ (14), *Egfr*$^{Wa5/+}$(15), and *Col2a1-Cre* (16) mouse strains were used as previously described. To generate *Col2a1-Cre Egfr*$^{Wa5/f}$ mice, we first bred *Col2a1-Cre* with *Egfr*$^{Wa5/+}$ to obtain *Col2a1-Cre Egfr*$^{Wa5/+}$, which were then crossed with *Egfr*$^{f/f}$ to generate *Col2a1-Cre Egfr*$^{Wa5/f}$ mice and their siblings *Col2a1-Cre Egfr*$^{f/+}$, *Egfr*$^{Wa5/f}$, and *Egfr*$^{f/+}$. *Col2a1-Cre Egfr*$^{Wa5/f}$ mice were identified by their wavy coat appearance and PCR genotyping of the *Cre* gene using primers 5′GAGTGATGAGGTTCGCAAGA3′ and 5′CTACACCAGAGACGGAAATC3′. All animal work performed in this report was approved by the Institutional Animal Care and Use Committee (IACUC) at the University of Pennsylvania.

Histological analyses, immunohistochemistry and in situ hybridization

To study growth plate morphology and calcification of rat bones, tibiae were dissected, fixed in 70% ethanol, processed for methylmethacrylate (MMA) embedding, and cut into 5 μm longitudinal sections using a Polycut-S motorized microtome (Reichert). Consecutive sections were processed for Goldner's trichrome staining and von Kossa staining. Proliferative and hypertrophic zones of the growth plate were measured on Goldner's trichrome-stained sections under the microscope at 100x magnification and calculated as an average of three measurements of the left, middle, and right regions of the growth plate. All sections were collected from the center of tibiae. The proliferative zone is defined as the area that contains flattened cells in a longitudinal and columnar arrangement. The hypertrophic zone is defined as the area from where the cell size starts to increase to where cartilage becomes bone (17,18).

For histological staining, tartrate-resistant acidic phosphatase (TRAP) staining and immunohistochemistry of rat bones, femurs or tibiae were fixed in 10% neutral buffered formalin overnight, washed under tap water, and then decalcified in 0.5 M EDTA (pH 7.4) for 3 weeks prior to processing and embedding in paraffin. Six μm-thick sections were cut for analyses. For Safranin O staining, sections were stained with hematoxylin, followed by 0.001% (wt/vol) fast green and 0.1% (wt/vol) Safranin O. For TRAP staining, sections were stained using a leukocyte acid phosphatase kit (Sigma-Aldrich). TRAP-positive cells at the COJ and in the primary spongiosa were counted under the microscope at 100x

magnification. For immunohistochemistry, sections were deparaffinized and washed in PBS. After antigen retrieval, endogenous peroxidase activity was quenched in 3% H_2O_2 for 15 min and washed in PBS. Sections were then blocked in blocking serum at room temperature for 1 h and incubated with a primary antibody at 4°C overnight. After washed in PBS, sections were incubated with a biotinylated secondary antibody and then an avidin-biotinylated horseradish peroxidase complex (Vectastain ABC kit, Vector laboratories) according to the manufacturer's directions. Finally, peroxidase activity was revealed by immersion in DAB (Dako). The following primary antibodies were used: rabbit anti-Ki67 antibody (Santa Cruz), rabbit anti-p57 antibody (Abcam), rabbit anti-EGFR antibody (Abcam), rabbit anti-type II collagen antibody (Abcam) and rabbit anti-Col2-3/4C (MMP13-generated type II collagen cleavage fragment) antibody (a gift from Dr. John S. Mort). For Bromodeoxyuridine (BrdU) staining, rats were intraperitoneally injected with BrdU at a dose of 100 μg/g body weight 2 h before euthanization. The staining was carried out on paraffin sections using a BrdU staining kit (Invitrogen) according to the manufacturer's directions.

In situ hybridization of paraffin sections processed from rat tibiae were performed as described previously (19). Highly conserved regions between mouse and rat cDNAs (over 93% of homology) were used as templates to generate probes: a 515bp mouse *collagen 10a1* (1302-1816; NM _009925) and a 723 bp mouse *Mmp13* (11-744; BC125320).

To study mouse growth plate morphology, tibiae were dissected from P5 pups of *Col2a1-Cre Egfr*$^{Wa5/f}$ mice and their siblings and processed for paraffin sections, Sections were stained by hematoxylin and eosin (H&E) and measured for lengths of proliferative and hypertrophic zones as described above.

Micro-computed tomography (microCT) measurement

The femurs were subjected to ex vivo microCT analyses (Skyscan 1172 high resolution microCT, Skyscan). To study the trabecular architecture of the distal femoral metaphysis, primary and secondary spongiosa areas, corresponding to 0.5 to 2.3 mm and 2.3 to 3.8 mm, respectively, below the lowest point of growth plate, were scanned at 10 μm resolution and analyzed using 3D analysis.

Growth plate tissue harvest, RNA and protein analyses

Rat tibiae were dissected free of soft tissue and their proximal ends, containing the growth plate, were cut longitudinally into approximately 0.5 mm-thick sections using a #22 surgical scalpel blade. Only those sections obtained from the center of tibiae (approximately 3-4 sections per tibia) were used for the microdissection. Under a dissection microscope, perichondrum and epiphyseal bone were first removed from these sections and growth plate cartilage was then carefully dissected out from the metaphyseal bone at the area just above the COJ (a fine red line) with a #15 surgical scalpel blade. As shown in supplemental Fig. 1, cartilage harvested by this method contained only chondrocytes and excluded cells located at the COJ and subchondral bone area. Growth plate tissues from the same bone were combined and processed for the following analyses.

To obtain RNA, growth plate tissue was homogenized in Tri Reagent (Sigma-Aldrich) followed by total RNA isolation and purification. A Taqman® Reverse Transcription kit (Applied Biosystems) was used to reverse transcribe mRNA into cDNA. Following this, quantitative real-time PCR (qRT-PCR) was performed using Power SYBR® Green PCR Master Mix kit (Applied Biosystems). The primer sequences for the genes used in this study are listed in a supplemental table. Relative expression was calculated for each gene by the $2^{-\Delta\Delta C_T}$ method with β-actin for normalization.

To obtain protein, growth plate tissue was ground in a liquid nitrogen-cooled pestle with a mortar and then dissolved in RIPA buffer (Santa Cruz). Equal amounts of protein lysates (30 μg per lane) were resolved by SDS/PAGE on 10% polyacrylamide gels, transferred to polyvinylidene difluoride membranes (Hybone-P, Amersham Biosciences), and blotted with rabbit anti-MMP9, anti-MMP13, anti-MMP14 antibodies (Abcam), anti-CGGVDIPEN (MMP-generated aggrecan cleavage fragment, a gift from Dr. John S. Mort) antibody at 4°C, or mouse anti-β-actin antibody (Santa Cruz) at 4°C overnight. After incubation with horseradish peroxidase-conjugated secondary antibody, blots were developed by enhanced chemiluminescence (ECL, GE Healthcare) following the manufacturer's protocol, and visualized by exposure to X-ray film (Eastman Kodak).

Alternatively, total protein lysates (15 μg) were mixed with 2 x sample buffer (4% SDS, 25% glycerol, 0.01% bromophenol blue and 62.5mM Tris, pH 6.8) and loaded without boiling onto a 10% acrylamide gel copolymerized with 1 mg/ml gelatin (Sigma-Aldrich). After running at 100 V for 1.5 h at 4 °C under non-reducing condition, the gel was washed twice in 2.5% Triton X-100 for 30 min to allow enzyme renaturation and then incubated in development buffer (Bio-Rad) at 37°C for 5 h. The gel was stained with 0.5% Coomassie blue R-250 (Thermo Scientific) for 1 h and destained in 40% methanol-10% acetic acid solution until evidence of proteolytic activity appeared as clear bands against the blue background.

Primary chondrocytes

Primary epiphyseal chondrocytes were isolated from the distal femoral, proximal and distal tibial condyles of 1- to 3-day-old Sprague-Dawley rats. Briefly, epiphyseal condyles were dissected, cleaned of connective tissue, and digested in type II collagenase solution (2.2 mg/ml in PBS, Invitrogen) at 37 °C with gentle agitation for 30 min. The condyles were collected and further digested with type II collagenase at 37 °C for 4 h. The supernatant was filtered and centrifuged to collect chondrocytes. Cells were plated at a density of 4×10^4 / cm^2 in 24-well plates in chondrogenic medium (DMEM/F12 medium with 10% fetal bovine serum, 50 μg/ml L-ascorbic acid, 1% glutamine, 100 μg/ml streptomycin and 100 U/ml penicillin). Two to three days later, when cells reached 90% confluence, cultures were given fresh media. The following day, cells were treated with 50 ng/ml recombinant human TGFα (Peprotech) and RNA and protein were harvested at indicated times for analysis.

Statistical analysis

All data were analyzed by independent Student's t-test assuming equal variances in each group or two-way ANOVA with a Bonferroni post-test. Animal number per group varied from 3-6. For cell culture experiments, all results are derived from experiments being repeated independently at least three times. A value of $p<0.05$ was considered significant. All data are expressed as mean ± sem.

Results

Inhibition of EGFR activity altered growth plate architecture

To study the role of EGFR in postnatal growth plate development, we administered an EGFR specific inhibitor, gefitinib, to 1-month-old rats for 7 days. Gefitinib-treated rats developed profound changes in the growth plate cartilage in both femurs and tibiae which were characterized by epiphyseal growth plate thickening and accumulation of hypertrophic chondrocytes (Fig. 1A and B). In these animals, we observed an overall 2.0-fold increase in the tibial growth plate length. This is mainly due to a striking increase in the length of hypertrophic zone (2.3-fold). There is no significant change in the length of the proliferative zone (1.2-fold increase, $p=0.07$) (Fig. 1C, D, and G). The enlargement of the hypertrophic

zone is mainly due to an increase in the number of chondrocytes but not an increase of cell size since the cell number per length remains the same (Fig.1H). The expansion of the hypertrophic zone was also confirmed by Safranin O staining which showed less staining intensity in the hypertrophic zone compared to the proliferative zone (Fig. 1E and F). In addition, immunostaining for Ki67, a marker for replicating cells, and p57, a marker for cell cycle exit, as well as in situ hybridization for Col10a1, a hypertrophic zone marker, further demonstrated that the elongation of growth plate in gefitinib-treated rats is mainly due to the expansion of the hypertropic zone (supplemental Fig. 2). This change in the growth plate was reversible since the length of the growth plate returned to normal one week after withdrawal of the EGFR inhibitor (data not shown). A similar phenotype was also noticed with rats treated with another EGFR-specific inhibitor, erlotinib (data not shown), confirming that this growth plate phenotype results from the loss of EGFR activity. In addition, we observed a small but significant decrease in the long bone length (for tibia, vehicle: 22.3 ± 0.2 mm vs. gefitinib: 20.5 ± 0.3 mm, p=0.02; for femur, vehicle: 25.7 ± 0.4 mm vs. gefitinib: 24.1 ± 0.3 mm, p=0.03, n=3-6/group) after 7 days of treatment.

The primary spongiosa of metaphyseal bone underneath the growth plate is derived directly from the hypertrophic zone through a bone modeling process. In normal rats, bone spicules in this area were extended from the chondrocyte columns and parallel to each other. However, gefitinib-treated rats had shorter bone spicules with irregular shapes (Fig. 2A and B). Interestingly, we noticed that there were more cartilage remnants in the bone spicules (light blue areas in Fig. 2A) in gefitinib-treated rats compared to vehicle-treated rats, implying that gefitinib delays the conversion of cartilage matrix into bone matrix.

MicroCT imaging further confirmed this phenomenon and the expansion of the growth plate (Fig. 2B). Quantitative analyses showed that the bone volume in the primary spongiosa was significantly decreased by 14% in the tibiae of gefitinib-treated rats (Fig. 2C). This was mainly due to an elevation in trabecular separation (22%) and a reduction in trabecular number (14%). The trabecular thickness was not changed in this area. In the secondary spongiosa where bone remodeling occurs, we observed a larger decrease in bone volume (36%) with similar changes in trabecular separation (19% increase, not significant) and trabecular number (36%) (Fig. 2B and D). This result is consistent with our recent finding that gefitinib treatment decreases bone volume and inhibits bone formation in young mice (20). Overall, these data indicate that postnatal long bone growth is affected by the loss of EGFR activity.

Gefitinib treatment delayed cartilage mineralization

Next we investigated whether cartilage mineralization was altered in the growth plate of gefitinib-treated rats. In agreement with numerous reports, von Kossa staining revealed that about one-half to two-thirds of the hypertrophic zones in the growth plates of normal rats were calcified (supplemental Fig. 3A and B). However, after gefitinib treatment, only the last 2-3 rows of chondrocytes in the hypertrophic zones were mineralized (supplemental Fig. 3C and D). This enlargement of growth plate and delayed mineralization is reminiscent of osteomalacia, a disease caused by the depletion of calcium. However, we did not observe any changes in the serum calcium ion level (vehicle: 12.2 ± 0.7 mg/dl vs. gefitinib: 12.5 ± 0.2 mm, p=0.87, n=6/group). Moreover, no expanded osteoid was observed in the trabecular bone of gefitinib-treatemed animals (Fig. 1A, B and Fig. 2A), suggesting that this phenomenon is not a result of altered calcium homeostasis.

Growth plate chondrocytes express EGFR

We performed immunohistochemistry to identify the cells that express EGFR protein in the growth plate. As shown in supplemental Fig. 4A and B, strong EGFR expression was

detected in all chondrocytes within the growth plate, suggesting that growth plate chondrocytes are the primary target for gefitinib. In addition, we observed very weak to no EGFR staining in the endothelial cells (supplemental Fig. 4C) and multinucleated osteoclasts (supplemental Fig. 4D) and strong staining in osteoblasts (supplemental Fig. 4C) in the primary spongiosa underneath the growth plate. These data are in agreement with our previous report that osteoblasts express EGFR but osteoclast progenitors and mature osteoclasts do not bind EGF ligand and do not possess functional EGFR (21).

Chondrocyte proliferation and differentiation are unchanged in gefitinib-treated rats

The expansion of the growth plate in gefitinib-treated rats could be the result of increased chondrocyte cell proliferation or altered differentiation. The aforementioned data demonstrating that gefitinib expands the hypertrophic zone but has no effect on the length of the proliferative zone provided the first hint that gefitinib does not change the proliferation and differentiation of chondrocytes in vivo. To further test this, we labeled rats with BrdU. Tibiae harvested from gefitinib-treated rats contained a similar percentage of BrdU-positive cells in the proliferative zone (vehicle: 22.6 ± 1.7% vs. gefitinib: 22.4 ± 2.3%, n=3/group) and a similar length of BrdU-labeled area as vehicle-treated rats (Fig. 3A), indicating that the enlargement of the growth plate is not due to an increased proliferative capacity of chondrocytes.

We then examined chondrocyte differentiation by measuring the mRNA expression of stage-specific differentiation markers in the growth plate. Note that growth plate tissue was dissected from tibiae free of perichondrum and bone contamination as described in the “Materials and Methods”. The genes for aggrecan and type II collagen (Col2a1), Ihh, and type X collagen (Col10a1) are specifically expressed in the proliferative, prehypertrophic and hypertrophic zones, respectively. We found that while the expression of aggrecan, Col2a1 and Ihh was not changed, Col10a1 increased about 2-fold in gefitinib-treated rats (Fig. 3B), which is consistent with the enlarged hypertrophic zone in the gefitinib-treated rats and in agreement with the in situ data detecting Col10a1 mRNA expression in the growth plate (supplemental Fig. 2). Sox9 and Runx2 are two master transcription factors essential for growth plate development. Sox9 is expressed in proliferating and prehypertrophic zones (22) and important for the determination of chondrocyte fate and maintenance of chondrocyte proliferation (23), while Runx2 is required for chondrocyte maturation and terminal differentiation (23). We found that gefitinib-treated rats expressed similar levels of Sox9 and Runx2 mRNA in the growth plate compared to vehicle-treated animals (Fig. 3B). Taken together, our data strongly suggest that chondrocyte differentiation is not affected by EGFR inhibition.

Gefitinib-treated rats have normal angiogenesis at the COJ

Previous reports have shown that suppressing the expression or activity of VEGFa, an important regulator of angiogenesis during endochondral ossification, inhibits blood vessel invasion into the hypertrophic zone of long bone growth plates and results in the expansion of the hypertrophic zone (24). To test whether vascularization is impaired in our animal model, we used H&E staining to identify red blood cells and their associated blood vessels along the COJ. As shown in Fig. 3C, we did not observe any overt difference in the number, location, orientation, or morphology of blood vessels underneath the growth plate in gefitinib-treated rats when compared to vehicle-treated rats. This is consistent with our immunohistochemistry results that endothelial cells do not express EGFR (supplementary Fig. 4D) and suggests that angiogenesis is not directly impaired by gefitinib. qRT-PCR revealed that the mRNA expression of Vegfa, along with another angiogenesis factor transferrin (25), was increased about 5.3- and 4.8-fold, respectively, in the growth plate after gefitinib treatment, which is consistent with the expansion of hypertrophic zone.

Gefitinib treatment suppresses the ability of chondrocytes to support osteoclastogenesis at the COJ

Osteoclasts at the COJ play an essential role in endochondral ossification through secreting various proteinases to digest cartilage ECM for vascular invasion and conversion from cartilage matrix into bone matrix. Mice that are unable to generate osteoclasts also develop enlarged hypertrophic zones in their growth plates (26). We therefore assessed the number of osteoclasts along the COJ using TRAP staining. Notably, we observed a significant decrease in the number of TRAP-positive cells located just below the last row of terminally differentiated chondrocytes in the gefitinib group compared to the vehicle group (vehicle: 10.9 ± 1.0 cells/mm vs. gefitinib: 5.5 ± 0.7 cells/mm, p=0.01, n=6 rats/group). However, the number of TRAP-positive cells in the area 0-0.64 mm below the COJ was similar between these two groups (vehicle: 59.4 ± 5.4 cells/mm^2 vs. gefitinib: 58.0 ± 5.6 cells/mm^2, n=6 rats/group) (Fig. 4A).

The aforementioned immunohistochemisty data (supplemental Fig. 4D) and our previous report (21) demonstrate that osteoclasts are not direct targets for gefitinib. To understand how gefitinib treatment reduced the number of osteoclasts along the COJ, we compared the mRNA levels of receptor activator of nuclear factor kappa-B ligand (RANKL), a major determinant for osteoclastogenesis, and osteoprotegerin (OPG), a decoy receptor for RANKL, in the growth plate using qRT-PCR. Interestingly, we observed a 3.6-fold decrease in RANKL expression but no significant change in OPG expression (p=0.17) in the gefitinib group compared to control. These changes result in an overall 60% decrease in the RANKL/OPG ratio after gefitinib treatment (Fig. 4B). To determine whether these changes were due to the direct action of gefitinib on chondrocytes, we treated primary chondrocytes with TGFα to activate EGFR. qRT-PCR revealed that TGFα up-regulated RANKL expression but suppressed OPG expression, resulting in 1.8-, 5.0-, and 16.6-fold increase in the ratio of RANKL/OPG after 8, 24, and 48 h of treatment, respectively (Fig. 4C). Moreover, this regulation was completely abolished by the inhibition of EGFR activity (Fig. 4D). These data demonstrate that EGFR signaling is important for chondrocytes to support osteoclastogenesis at the COJ.

Inhibition of EGFR activity decreases matrix metalloproteinase (MMP9, 13 and 14) expression and ECM degradation

MMPs are members of a family of zinc-dependent proteolytic enzymes. Several of them are expressed at high levels in bone and cartilage and essential for the cleavage of cartilage ECM and remodeling of cartilage into bone. Blocking MMP activity either by a broad-spectrum inhibitor (27) or by knocking down specific MMP genes, such as MMP9 (28), 13 (29,30), and 14 (31), diminish matrix degradation and expand the growth plate. Interestingly, we found that the mRNA levels of these MMPs were significantly suppressed 3- to 4-fold in the growth plate of gefitinib-treated rats (Fig. 5A). Western blotting confirmed strong decreases at the protein level (Fig. 5B). Moreover, gelatin zymography showed that the activity of MMP9 (gelatinase B), in both pro and mature forms, was attenuated, while MMP2 (gelatinase A) activity was not affected (Fig. 5C). In situ hybridization further revealed that MMP13 gene expression in the terminally differentiated chondrocytes was dramatically suppressed by gefitinib (Fig. 5D).

To test whether the decrease in MMP expression lead to accumulation of intact collagen fibers, polarized light microscopy was used to quantify the intensity of birefringent collagen in the growth plate. In the vehicle group, we observed strong type I collagen birefringency in the primary spongiosa, most of which was aligned with bone spicules. However, the birefringency in the growth plate was weak and existed mostly in the longitudinal septa between columns of chondrocytes (Fig. 5E). Quantitative imaging analysis revealed that

there was a significant 2.2-fold increase in the intensity of birefringency in the growth plate of gefitinib-treated rats. Moreover, picrosirius red staining for collagen showed a similar increase in collagen birefringent intensity in the gefitinib group (data not shown). Type II collagen is the major collagen in the growth plate. Immunohistochemical staining showed an increase in type II collagen in the gefitinib-treated growth plate compared to the control (Fig. 5F). This increase is not due to an increase in gene expression because the mRNA level of Col2a1 was not changed (Fig. 3B).

Accumulation of ECM proteins due to decreases in MMP levels should be accompanied by reduced ECM degradation. Immunostaining for a neoepitope in the collagenase cleavage site in the 3/4 fragment of type II collagen indicated that there was decreased degraded type II collagen in the perilacunar surrounding of hypertrophic chondrocytes and at the COJ in the gefitinib group compared to the vehicle group (Fig. 5G). Importantly, degraded type II collagen staining at the COJ was decreased in the gefitinib-treated rats compared to the control. As shown in Fig. 5H, Western blot indicated that the amount of MMP-cleaved aggrecan fragment was also decreased in the growth plate of gefitinib-treated rats. Taken together, these data strongly suggest that ECM degradation is partially blunted by EGFR inhibition.

EGFR signaling stimulates MMP expression in primary chondrocytes

We next determined whether the decrease in MMP expression was due to a direct effect of gefitinib on the EGFR in chondrocytes. Primary chondrocytes were treated with TGFα to activate EGFR. qRT-PCR revealed that TGFα increased MMP9 mRNA 1.9-, 3.8-, and 12.8-fold at 8, 24, and 48 h, respectively, and increased MMP13 mRNA 1.7-, 3.3-, and 23.9-fold at 8, 24, and 48 h, respectively (Fig. 6A). However, MMP14 mRNA was only increased 1.6-fold at 48 h. Western blot analyses confirmed that the expression of MMP9, 13 and 14 was up-regulated at the protein level. This stimulation was completely abolished by gefitinib (Fig. 6B), indicating that TGFα regulation of MMPs is EGFR-dependent.

Mice deficient in chondrogenic EGFR activity have an enlarged hypertropic zone

In the above experiments, oral administration of the EGFR inhibitor to rats suppressed EGFR activity ubiquitously. To exclude the possibility that gefitinib might act on cells other than chondrocytes to affect growth plate development, we initially generated collagen2a1 promoter-driven Cre (*Col2a1-Cre*) $Egfr^{flox/flox}$ mice. In neonatal mice *Col2a1-Cre* was expressed in the chondrocytes of the long bone epiphysis (16). However, genotyping and Western blots with these mice revealed an incomplete deletion of *Egfr* alleles and no significant change in EGFR protein amount in the epiphyseal cartilage (supplemental Fig. 5). To further reduce the remaining EGFR activity, we introduced an EGFR dominant negative allele, Wa5 (15), and generated *Col2a1-Cre* $Egfr^{Wa5/f}$ mice. Previously, we have successfully used this strategy to characterize pre/osteoblast-specific EGFR null mice (20). Analyzing the long bone growth plate at P5 revealed that, while the Wa5 allele itself ($Egfr^{Wa5/f}$ mice) modestly increased the length of the hypertrophic zone (1.3-fold), introducing *Col2-Cre* further dramatically expanded the hypertrophic zone to 2.0-fold compared to $Egfr^{+/f}$ mice (Fig. 7A,B). These data strongly demonstrate that chondrogenic EGFR activity is essential for cartilage remodeling into bone. Consistent with the gefitinib-treated rat result, we did not observe any difference in the length of the proliferative zone in these mice (Fig.7), implying that the major reason for the expanded growth plate is also due to the delayed cartilage remodeling into bone.

Discussion

Significant skeletal defects have long been noticed in mouse models with abnormal EGFR activity. Recently, we reported that EGFR ligands stimulate osteoclastogenesis indirectly by suppressing OPG expression and enhancing MCP1 expression in differentiating osteoblasts (21). Furthermore, we demonstrated that EGFR is an anabolic regulator of bone formation that is important for the maintenance of a pool of mesenchymal stem cells and osteoprogenitors in bone (20). In this report, we demonstrated that EGFR signaling is also an important regulator of postnatal growth plate development and endochondral ossification. Blocking EGFR activity specifically with small molecule inhibitors dramatically expanded the length of the growth plate, particularly the hypertrophic zone, in rat long bones. While chondrocyte proliferation, differentiation, and angiogenesis at COJ were relatively normal, the removal of hypertrophic cartilage matrix by osteoclasts and MMPs was suppressed. Interestingly, the effect of the EGFR inhibitor on the growth plate is reversible, suggesting that normal cartilage matrix degradation is rapidly restored after the removal of EGFR inhibition. A similar growth plate phenomenon is also observed upon chondrocyte-specific inactivation of the *Egfr* gene in mice and in *Tgfα* null mice (Usmani et al., submitted), further confirming that EGFR signaling is critical for growth plate remodeling in long bones.

ECM degradation in the growth plate is an essential step in endochondral ossification. The growth plate contains an ECM mainly comprised of type II and type X collagens and the aggregating proteoglycan (aggrecan). To form new bone, hypertrophic chondrocytes and osteoclasts need to partially degrade the growth plate ECM at the COJ, generating space for osteoblasts to deposit bone matrix. MMPs, in particular MMP9, 13, and 14, are key enzymes involved in this process. MMP13, also named collagenase 3, is the major protease that degrades native type II collagen (32). MMP9 and 13 together are responsible for MMP-dependent aggrecan cleavage (30). MMP14, also named membrane-type I MMP (MT1-MMP), functions as a potent pericellular collagenase capable of degrading both type I and type II collagen (33) and is important for the formation of the secondary ossification center (31). Mice deficient in either MMP9, 13, or 14 all have an expanded hypertrophic zone in the growth plate during early postnatal bone growth due to impeded ECM degradation, a phenotype similar to our EGFR inhibitor-treated young rats. However, once MMP9 knockout or MMP13 knockout mice reach adulthood, the enlarged growth plate is no longer observed, likely due to the redundancy among the various proteases.

MMP9, 13, and 14 are expressed by cells in and surrounding the growth plate. MMP13 is mainly expressed in hypertrophic chondrocytes and osteoblasts (34). In situ hybridization and immunostaining indicate that cells with high MMP9 expression are osteoclasts (28,35) and TRAP-negative cells of unknown lineage beneath the hypertrophic cartilage (26). Meanwhile, MMP9 expression was also identified in the hypertrophic chondrocytes of mouse cartilage by immunostaining (36) and throughout the growth plate in 4-week-old rats by in situ hybridization (37). MMP14 is mainly expressed in the resting and proliferative zones while the hypertrophic zone showed little expression (38). MMP14 is also abundant in osteoclasts (39) and exhibits intense staining in the region beneath COJ (38). To avoid possible contamination of cells other than chondrocytes, we used a stereo microscope to dissect out the growth plate tissue from rat tibiae containing chondrocytes only but not osteoblasts, osteoclasts and other cells at COJ and confirmed the presence of only chondrocytes within our samples by histology. We demonstrate that those growth plate samples do express MMP9, 13 and 14 mRNA and protein and that this expression was attenuated by blocking EGFR activity. This is consistent with a previous study that showed severe craniofacial defects in *Egfr* null mice and diminished MMP secretion from mandibular explants from these animals (7). We show that the decreases in MMP amounts

are correlated to the accumulation of collagen and decreases in degraded aggrecan and type II collagen products in the growth plate. Further in vitro experiments revealed that TGFα stimulates MMP9, 13 and 14 expression in primary chondrocytes via activation of EGFR. This result suggests that gefitinib directly acts on chondrocytes in vivo to block MMP expression. Taken together, these data demonstrate that EGFR signaling is critical for maintaining the expression of these three MMPs in the growth plate and subsequently promoting ECM degradation.

In addition to the diminished expression of MMPs, our data suggest that delayed osteoclast recruitment and differentiation at COJ could be another mechanism for the expansion of the growth plate after gefitinib treatment. We found that, while the osteoclast number in the primary spongiosa was unchanged, the osteoclast number at the COJ was significantly decreased in gefitinib-treated rats. A previous report showed that *Egfr*$^{-/-}$ mice have delayed endochondral ossification and an enlarged hypertrophic zone in the growth plate (8). At E16.5, wild type mice had already formed primary ossification centers while *Egfr*$^{-/-}$ mice still had a continuous cartilage anlage in the middle of the long bone. Wang et al. noticed that, at that stage, the number of osteoclasts adjacent to the hypertrophic cartilage in *Egfr*$^{-/-}$ mice was less than that in the bone marrow of wild type mice and concluded that the impaired endochondral ossification in *Egfr*$^{-/-}$ mice is due to the loss of EGFR signaling in osteoclasts. However, their conclusion cannot explain their observation that there was no difference in osteoclast number in the bone marrow at later stage (E18.5) when the primary ossification center was formed and the enlarged hypertrophic zone was still prominent in the *Egfr*$^{-/-}$ mice. It also cannot explain why we did not observe any change in osteoclast number in the primary spongiosa after gefitinib treatment. In addition, our previous data showed that osteoclastic lineage cells do not express functional EGFR (21) and our current immunostaining showed very weak EGFR staining in osteoclasts. Importantly, we also show that chondrocyte-specific inactivation of EGFR (*Col2a1-Cre Egfr*$^{Wa5/f}$ mice) caused similar enlargement of the hypertrophic zone postnatally. All these data strongly suggest that an additional indirect mechanism might be responsible for mediating the effects of EGFR on osteoclasts.

Here, we attribute the decrease in osteoclast number to a decrease in the RANKL/OPG ratio in the growth plate. RANKL and OPG are expressed by hypertrophic chondrocytes in the growth plate during embryonic development (40). It is known that vitamin D3 can regulate RANKL expression in chondrocytes to promote osteoclast formation in vivo (41). In vitro coculture experiments demonstrate that chondrocytes are capable of supporting osteoclastogenesis directly (42). Since RANKL/OPG is stimulated by TGFα in primary chondrocytes, we conclude that hypertrophic chondrocytes are the major determinant of osteoclast formation at the COJ and EGFR signaling in chondrocytes is essential for this process. Notably, *Tgfa* null mice also display reduced expression of RANKL and MMP13 in the cartilage (Usmani et al., submitted).

In vitro chondrocyte culture experiments have demonstrated that activation of EGFR signaling strongly stimulates chondrocyte proliferation (43,44), inhibits chondrogenesis (45), and suppresses the expression of chondrocyte matrix genes (46). Surprisingly, we found that gefitinib treatment did not alter chondrocyte proliferation and differentiation in vivo. Since immunostaining shows EGFR expression throughout the growth plate, we reason that EGFR might be activated differentially within these zones. A previous study of growth plate in chickens suggests that EGF and TGFα are expressed in the prehypertrophic and hypertrophic zones but not in the proliferative zone during early postnatal growth (47). Expression of EGF-like ligands only in mature chondrocytes can explain why inhibition of EGFR activity affects RANKL and MMP expression in hypertrophic chondrocytes but has

no effect on chondrocyte proliferation and differentiation. Further analysis to locate the activated EGFR will be required to confirm this hypothesis.

In conclusion, our studies reveal a novel critical role of EGFR in growth plate cartilage ECM remodeling. We demonstrate that EGFR signaling regulates matrix degradation directly by stimulating growth plate chondrocytes to express MMPs and indirectly by supporting osteoclastogenesis at the COJ (Fig. 7C). These two mechanisms might be complementarily interplayed. It is possible that gefitinib-induced delay in growth plate mineralization is secondary to the defects in matrix degradation since MMP 9 and 13 are components of matrix vesicles (48), which are responsible for cartilage calcification, and MMP13 activity is important for chondrocyte mineralization in vitro (49). To date, no defects in human bone or cartilage growth have been linked to alterations in the EGFR pathway. However, in chickens, EGF may play a role in tibial dyschondroplasia, a chicken growth plate disorder that bears resemblance to human diseases such as osteochondrosis and metaphyseal chondroplasia. Chickens with this disorder show overexpression of EGF in the proliferating zone and diminished expression of EGF and TGFα in the hypertrophic zone (47). Future investigations are needed to understand how EGFR regulates endochondral ossification and whether alterations in this pathway lead to human long bone growth defects.

Supplementary Material

Refer to Web version on PubMed Central for supplementary material.

Acknowledgments

The authors would like to thank Drs. Charles Clark and Olena Jacenko at the University of Pennsylvania and Dr. Maurizio Pacifici at the Children's Hospital of Philadelphia for providing critical comments and technical advice on this project and Dr. John S. Mort at Shriners Hospital for Children (Montreal, Canada) for degraded type II collagen and aggrecan antibodies. Also, special thanks to Genentech for providing erlotinib for our studies.

Funding sources: This study was supported by NIH grant DK071988 (to LQ) and CIHR (Canadian Institutes of Health Research) grant 86574 (to FB).

References

1. Karsenty G, Wagner EF. Reaching a genetic and molecular understanding of skeletal development. Dev Cell. 2002; 2(4):389–406. [PubMed: 11970890]
2. Kronenberg HM. Developmental regulation of the growth plate. Nature. 2003; 423(6937):332–6. [PubMed: 12748651]
3. Citri A, Yarden Y. EGF-ERBB signalling: towards the systems level. Nat Rev Mol Cell Biol. 2006; 7(7):505–16. [PubMed: 16829981]
4. Miettinen PJ, Berger JE, Meneses J, Phung Y, Pedersen RA, Werb Z, Derynck R. Epithelial immaturity and multiorgan failure in mice lacking epidermal growth factor receptor. Nature. 1995; 376(6538):337–41. [PubMed: 7630400]
5. Sibilia M, Wagner EF. Strain-dependent epithelial defects in mice lacking the EGF receptor. Science. 1995; 269(5221):234–8. [PubMed: 7618085]
6. Threadgill DW, Dlugosz AA, Hansen LA, Tennenbaum T, Lichti U, Yee D, LaMantia C, Mourton T, Herrup K, Harris RC, et al. Targeted disruption of mouse EGF receptor: effect of genetic background on mutant phenotype. Science. 1995; 269(5221):230–4. [PubMed: 7618084]
7. Miettinen PJ, Chin JR, Shum L, Slavkin HC, Shuler CF, Derynck R, Werb Z. Epidermal growth factor receptor function is necessary for normal craniofacial development and palate closure. Nat Genet. 1999; 22(1):69–73. [PubMed: 10319864]
8. Wang K, Yamamoto H, Chin JR, Werb Z, Vu TH. Epidermal growth factor receptor-deficient mice have delayed primary endochondral ossification because of defective osteoclast recruitment. J Biol Chem. 2004; 279(51):53848–56. [PubMed: 15456762]

9. Sibilia M, Wagner B, Hoebertz A, Elliott C, Marino S, Jochum W, Wagner EF. Mice humanised for the EGF receptor display hypomorphic phenotypes in skin, bone and heart. Development. 2003; 130(19):4515–25. [PubMed: 12925580]
10. Fisher MC, Clinton GM, Maihle NJ, Dealy CN. Requirement for ErbB2/ErbB signaling in developing cartilage and bone. Dev Growth Differ. 2007; 49(6):503–13. [PubMed: 17555517]
11. Schneider MR, Mayer-Roenne B, Dahlhoff M, Proell V, Weber K, Wolf E, Erben RG. High cortical bone mass phenotype in betacellulin transgenic mice is EGFR dependent. J Bone Miner Res. 2009; 24(3):455–67. [PubMed: 19049329]
12. Chan SY, Wong RW. Expression of epidermal growth factor in transgenic mice causes growth retardation. J Biol Chem. 2000; 275(49):38693–8. [PubMed: 11001946]
13. Harari PM, Allen GW, Bonner JA. Biology of interactions: antiepidermal growth factor receptor agents. J Clin Oncol. 2007; 25(26):4057–65. [PubMed: 17827454]
14. Lee TC, Threadgill DW. Generation and validation of mice carrying a conditional allele of the epidermal growth factor receptor. Genesis. 2009; 47(2):85–92. [PubMed: 19115345]
15. Lee D, Cross SH, Strunk KE, Morgan JE, Bailey CL, Jackson IJ, Threadgill DW. Wa5 is a novel ENU-induced antimorphic allele of the epidermal growth factor receptor. Mamm Genome. 2004; 15(7):525–36. [PubMed: 15366372]
16. Ovchinnikov DA, Deng JM, Ogunrinu G, Behringer RR. Col2a1-directed expression of Cre recombinase in differentiating chondrocytes in transgenic mice. Genesis. 2000; 26(2):145–6. [PubMed: 10686612]
17. Gillespie JR, Ulici V, Dupuis H, Higgs A, Dimattia A, Patel S, Woodgett JR, Beier F. Deletion of glycogen synthase kinase-3beta in cartilage results in up-regulation of glycogen synthase kinase-3 alpha protein expression. Endocrinology. 2011; 152(5):1755–66. [PubMed: 21325041]
18. van der Eerden BC, Karperien M, Wit JM. Systemic and local regulation of the growth plate. Endocr Rev. 2003; 24(6):782–801. [PubMed: 14671005]
19. Koyama E, Young B, Nagayama M, Shibukawa Y, Enomoto-Iwamoto M, Iwamoto M, Maeda Y, Lanske B, Song B, Serra R, Pacifici M. Conditional Kif3a ablation causes abnormal hedgehog signaling topography, growth plate dysfunction, and excessive bone and cartilage formation during mouse skeletogenesis. Development. 2007; 134(11):2159–69. [PubMed: 17507416]
20. Zhang X, Tamasi J, Lu X, Zhu J, Chen H, Tian X, Lee TC, Threadgill DW, Kream BE, Kang Y, Partridge NC, Qin L. Epidermal growth factor receptor plays an anabolic role in bone metabolism in vivo. J Bone Miner Res. 2011; 26(5):1022–34. [PubMed: 21542005]
21. Zhu J, Jia X, Xiao G, Kang Y, Partridge NC, Qin L. EGF-like ligands stimulate osteoclastogenesis by regulating expression of osteoclast regulatory factors by osteoblasts: implications for osteolytic bone metastases. J Biol Chem. 2007; 282(37):26656–64. [PubMed: 17636266]
22. Zhao Q, Eberspaecher H, Lefebvre V, De Crombrugghe B. Parallel expression of Sox9 and Col2a1 in cells undergoing chondrogenesis. Dev Dyn. 1997; 209(4):377–86. [PubMed: 9264261]
23. Lefebvre V, Smits P. Transcriptional control of chondrocyte fate and differentiation. Birth Defects Res C Embryo Today. 2005; 75(3):200–12. [PubMed: 16187326]
24. Zelzer E, Olsen BR. Multiple roles of vascular endothelial growth factor (VEGF) in skeletal development, growth, and repair. Curr Top Dev Biol. 2005; 65:169–87. [PubMed: 15642383]
25. Carlevaro MF, Albini A, Ribatti D, Gentili C, Benelli R, Cermelli S, Cancedda R, Cancedda FD. Transferrin promotes endothelial cell migration and invasion: implication in cartilage neovascularization. J Cell Biol. 1997; 136(6):1375–84. [PubMed: 9087450]
26. Ortega N, Wang K, Ferrara N, Werb Z, Vu TH. Complementary interplay between matrix metalloproteinase-9, vascular endothelial growth factor and osteoclast function drives endochondral bone formation. Dis Model Mech. 2010; 3(3-4):224–35. [PubMed: 20142327]
27. Renkiewicz R, Qiu L, Lesch C, Sun X, Devalaraja R, Cody T, Kaldjian E, Welgus H, Baragi V. Broad-spectrum matrix metalloproteinase inhibitor marimastat-induced musculoskeletal side effects in rats. Arthritis Rheum. 2003; 48(6):1742–9. [PubMed: 12794843]
28. Vu TH, Shipley JM, Bergers G, Berger JE, Helms JA, Hanahan D, Shapiro SD, Senior RM, Werb Z. MMP-9/gelatinase B is a key regulator of growth plate angiogenesis and apoptosis of hypertrophic chondrocytes. Cell. 1998; 93(3):411–22. [PubMed: 9590175]

29. Inada M, Wang Y, Byrne MH, Rahman MU, Miyaura C, Lopez-Otin C, Krane SM. Critical roles for collagenase-3 (Mmp13) in development of growth plate cartilage and in endochondral ossification. Proc Natl Acad Sci U S A. 2004; 101(49):17192–7. [PubMed: 15563592]

30. Stickens D, Behonick DJ, Ortega N, Heyer B, Hartenstein B, Yu Y, Fosang AJ, Schorpp-Kistner M, Angel P, Werb Z. Altered endochondral bone development in matrix metalloproteinase 13-deficient mice. Development. 2004; 131(23):5883–95. [PubMed: 15539485]

31. Zhou Z, Apte SS, Soininen R, Cao R, Baaklini GY, Rauser RW, Wang J, Cao Y, Tryggvason K. Impaired endochondral ossification and angiogenesis in mice deficient in membrane-type matrix metalloproteinase I. Proc Natl Acad Sci U S A. 2000; 97(8):4052–7. [PubMed: 10737763]

32. Mitchell PG, Magna HA, Reeves LM, Lopresti-Morrow LL, Yocum SA, Rosner PJ, Geoghegan KF, Hambor JE. Cloning, expression, and type II collagenolytic activity of matrix metalloproteinase-13 from human osteoarthritic cartilage. J Clin Invest. 1996; 97(3):761–8. [PubMed: 8609233]

33. Wagenaar-Miller RA, Engelholm LH, Gavard J, Yamada SS, Gutkind JS, Behrendt N, Bugge TH, Holmbeck K. Complementary roles of intracellular and pericellular collagen degradation pathways in vivo. Mol Cell Biol. 2007; 27(18):6309–22. [PubMed: 17620416]

34. Tuckermann JP, Pittois K, Partridge NC, Merregaert J, Angel P. Collagenase-3 (MMP-13) and integral membrane protein 2a (Itm2a) are marker genes of chondrogenic/osteoblastic cells in bone formation: sequential temporal, and spatial expression of Itm2a, alkaline phosphatase, MMP-13, and osteocalcin in the mouse. J Bone Miner Res. 2000; 15(7):1257–65. [PubMed: 10893674]

35. Engsig MT, Chen QJ, Vu TH, Pedersen AC, Therkidsen B, Lund LR, Henriksen K, Lenhard T, Foged NT, Werb Z, Delaisse JM. Matrix metalloproteinase 9 and vascular endothelial growth factor are essential for osteoclast recruitment into developing long bones. J Cell Biol. 2000; 151(4):879–89. [PubMed: 11076971]

36. Miao D, Bai X, Panda DK, Karaplis AC, Goltzman D, McKee MD. Cartilage abnormalities are associated with abnormal Phex expression and with altered matrix protein and MMP-9 localization in Hyp mice. Bone. 2004; 34(4):638–47. [PubMed: 15050894]

37. Takahashi I, Onodera K, Bae JW, Mitani H, Sasano Y. Age-related changes in the expression of gelatinase and tissue inhibitor of metalloproteinase genes in mandibular condylar, growth plate, and articular cartilage in rats. J Mol Histol. 2005; 36(5):355–66. [PubMed: 16208432]

38. Shi J, Son MY, Yamada S, Szabova L, Kahan S, Chrysovergis K, Wolf L, Surmak A, Holmbeck K. Membrane-type MMPs enable extracellular matrix permissiveness and mesenchymal cell proliferation during embryogenesis. Dev Biol. 2008; 313(1):196–209. [PubMed: 18022611]

39. Andersen TL, del Carmen Ovejero M, Kirkegaard T, Lenhard T, Foged NT, Delaisse JM. A scrutiny of matrix metalloproteinases in osteoclasts: evidence for heterogeneity and for the presence of MMPs synthesized by other cells. Bone. 2004; 35(5):1107–19. [PubMed: 15542036]

40. Kishimoto K, Kitazawa R, Kurosaka M, Maeda S, Kitazawa S. Expression profile of genes related to osteoclastogenesis in mouse growth plate and articular cartilage. Histochem Cell Biol. 2006; 125(5):593–602. [PubMed: 16283360]

41. Masuyama R, Stockmans I, Torrekens S, Van Looveren R, Maes C, Carmeliet P, Bouillon R, Carmeliet G. Vitamin D receptor in chondrocytes promotes osteoclastogenesis and regulates FGF23 production in osteoblasts. J Clin Invest. 2006; 116(12):3150–9. [PubMed: 17099775]

42. Usui M, Xing L, Drissi H, Zuscik M, O'Keefe R, Chen D, Boyce BF. Murine and chicken chondrocytes regulate osteoclastogenesis by producing RANKL in response to BMP2. J Bone Miner Res. 2008; 23(3):314–25. [PubMed: 17967138]

43. Halevy O, Schindler D, Hurwitz S, Pines M. Epidermal growth factor receptor gene expression in avian epiphyseal growth-plate cartilage cells: effect of serum, parathyroid hormone and atrial natriuretic peptide. Mol Cell Endocrinol. 1991; 75(3):229–35. [PubMed: 1827415]

44. Hiraki Y, Inoue H, Kato Y, Fukuya M, Suzuki F. Combined effects of somatomedin-like growth factors with fibroblast growth factor or epidermal growth factor in DNA synthesis in rabbit chondrocytes. Mol Cell Biochem. 1987; 76(2):185–93. [PubMed: 3499565]

45. Yoon YM, Oh CD, Kim DY, Lee YS, Park JW, Huh TL, Kang SS, Chun JS. Epidermal growth factor negatively regulates chondrogenesis of mesenchymal cells by modulating the protein kinase

C-alpha, Erk-1, and p38 MAPK signaling pathways. J Biol Chem. 2000; 275(16):12353–9. [PubMed: 10766877]

46. Appleton CT, Usmani SE, Bernier SM, Aigner T, Beier F. Transforming growth factor alpha suppression of articular chondrocyte phenotype and Sox9 expression in a rat model of osteoarthritis. Arthritis Rheum. 2007; 56(11):3693–705. [PubMed: 17968906]
47. Ren P, Rowland GN 3rd, Halper J. Expression of growth factors in chicken growth plate with special reference to tibial dyschondroplasia. J Comp Pathol. 1997; 116(3):303–20. [PubMed: 9147248]
48. D'Angelo M, Billings PC, Pacifici M, Leboy PS, Kirsch T. Authentic matrix vesicles contain active metalloproteases (MMP). a role for matrix vesicle-associated MMP-13 in activation of transforming growth factor-beta. J Biol Chem. 2001; 276(14):11347–53. [PubMed: 11145962]
49. Wu CW, Tchetina EV, Mwale F, Hasty K, Pidoux I, Reiner A, Chen J, Van Wart HE, Poole AR. Proteolysis involving matrix metalloproteinase 13 (collagenase-3) is required for chondrocyte differentiation that is associated with matrix mineralization. J Bone Miner Res. 2002; 17(4):639–51. [PubMed: 11918221]

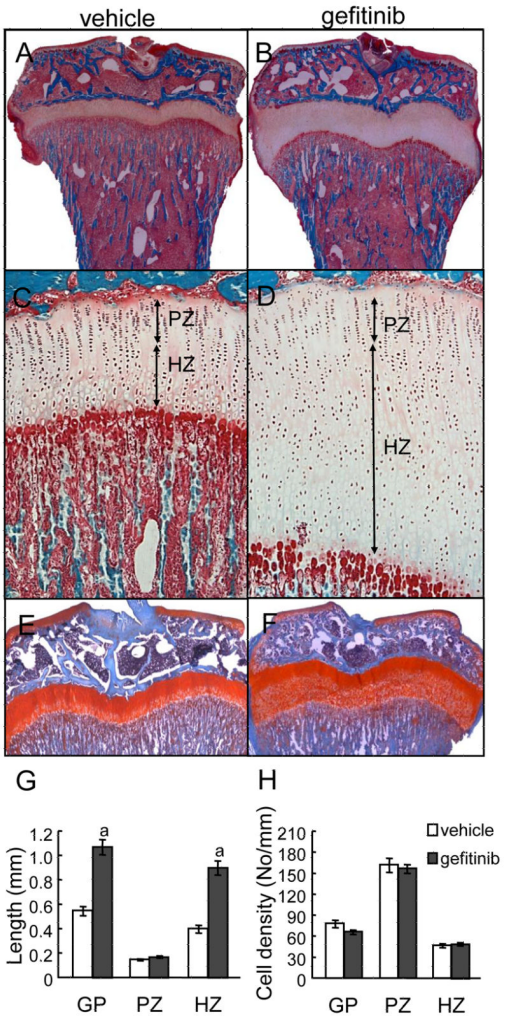

Figure 1. In vivo inhibition of EGFR activity expands the long bone growth plates

One-month-old rats were treated with either vehicle (A,C,E) or gefitinib (B,D,F) for 7 days and their tibiae were processed for MMA sections (A-D) or paraffin sections (E-F) for histological examination. Staining of the bone with Goldner's trichrome staining showed a striking enlargement of the growth plate, particularly the hypertrophic zone, in the gefitinib-treated animals (the whole bone at low magnification (A-B) and the growth plate region at high magnification (C-D)). PZ: proliferative zone; HZ: hypertrophic zone. (E-F) Safranin O staining confirms the increase in the length of hypertrophic zone. (G) Quantification of the lengths of whole growth plate (GP) and each zones. n=5/group. a: $p<0.001$ vs. vehicle. (H) Quantification of chondrocyte number along the longitudinal length of cartilage.

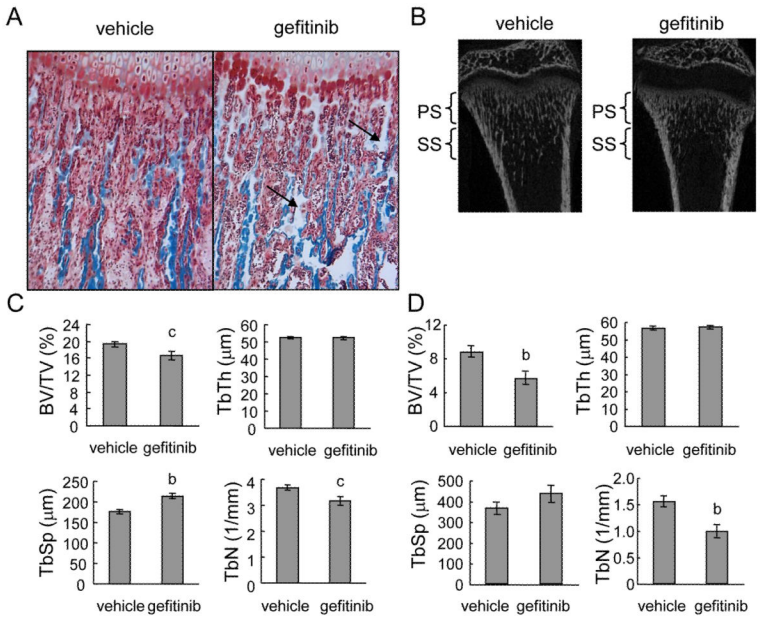

Figure 2. Gefitinib treatment expands the growth plate and decreases bone volume in the primary spongiosa (PS) and secondary spongiosa (SS) of rat long bones

(A)Magnified image of COJ and primary spongiosa in Goldner's trichrome-stained rat tibiae treated with vehicle or gefitinib. Arrows indicate cartilage remnants (light blue) in the bone spicules. (B) MicroCT images of longitudinal sections of distal femurs of vehicle- and gefitinib-treated rats. (C) Structural parameters of trabecular bone in the primary spongiosa. (D) Structural parameters of trabecular bone in the secondary spongiosa. BV/TV: trabecular bone volume/tissue volume; TbTh: trabecular thickness; TbSp: trabecular separation; TbN: trabecular number. n=6/group. b: $p<0.01$; c: $p<0.05$ vs. vehicle.

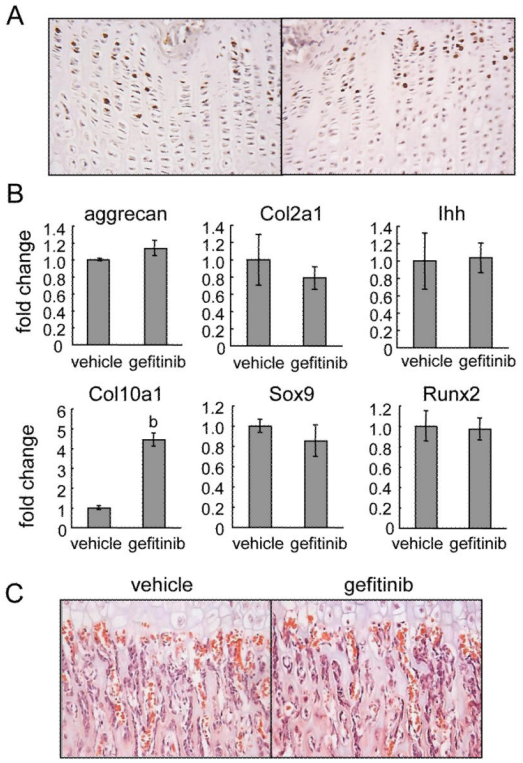

Figure 3. Gefitinib treatment does not alter chondrocyte proliferation, differentiation and vascular invasion

(A) BrdU incorporation (brown staining) in the proliferative zone of growth plates from vehicle- and gefitinib-treated rats. (B) qRT-PCR analysis of gene expression of stage-specific chondrocyte markers (*aggrecan, col2a1, Ihh*, and *Col10a1*) and transcription factors (*Sox9* and *Runx2*). b: $p<0.01$ vs. vehicle. (C) H&E staining of rat tibiae show that there is no overt difference in localization, size or morphology of blood vessels in the gefitinib-treated rats compared to vehicle-treated rats. Red blood cells are stained red with no blue nuclei.

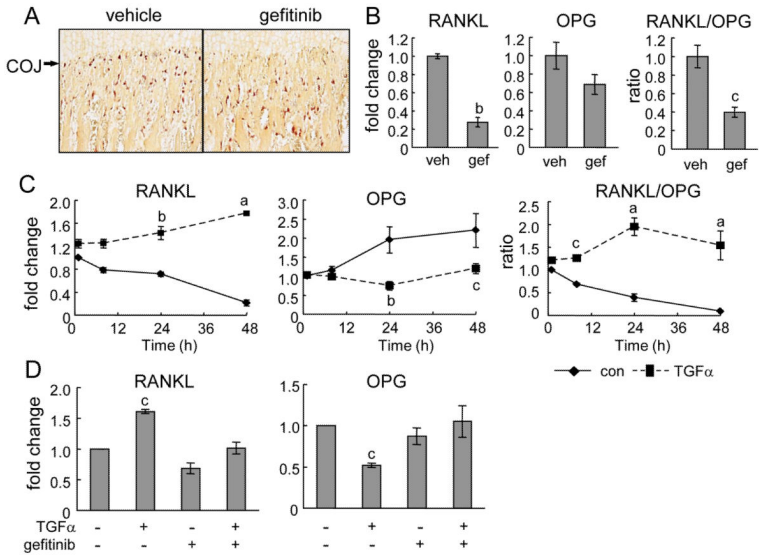

Figure. 4. Osteoclast differentiation at the COJ iss delayed in the gefitinib-treated rats

(A) TRAP staining (red) of rat tibiae reveals that gefitinib-treated rats have fewer osteoclasts at the COJ but comparable osteoclast number in the primary spongiosa underneath the junction. (B) qRT-PCR measurement of mRNA expression of RANKL and OPG in the growth plate dissected from vehicle- and gefitinib-treated rats. (C) qRT-PCR measurement of mRNA expression of RANKL and OPG in primary chondrocytes treated by TGFα for indicated time points. The mRNA level of the control group at 1 h was set to 1. (D) qRT-PCR demonstrates that 5 μM gefitinib abolishes the effects of 24 h of TGFα treatment on RANKL and OPG expression in primary chondrocytes. a: $p<0.001$; b: $p<0.01$; c: $p<0.05$ vs. control.

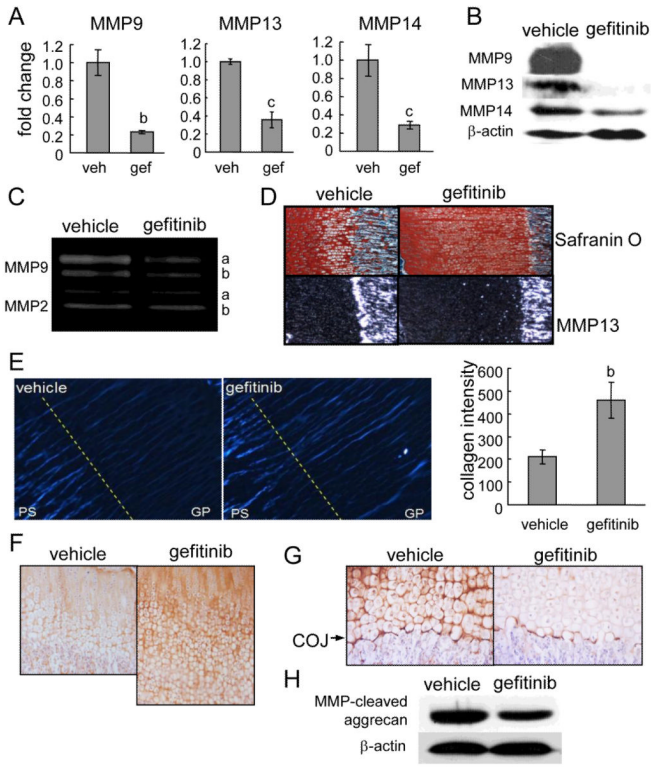

Figure 5. Blocking EGFR activity suppresses the expression of MMPs and ECM degradation in growth plate

(A) qRT-PCR analyses of MMP mRNA expression in the growth plate tissues from vehicle- and gefitinib-treated rats. b: $p<0.01$; c; $p<0.05$ vs. vehicle. (B) Western blotting shows that the protein levels of MMP9, 13, and 14 in the growth plates from gefitinib-treated rats were decreased to 7.9±2.1%, 14.0±12.6%, and 39.2±10.5%, respectively, of those from vehicle group as measured by densitometric analyses. (C) In situ hybridization reveals a decrease of MMP13 expression in the gefitinib-treated growth plate. (D) Gelatin zymography analysis of protein lysates from growth plate further confirms the decrease of MMP9 activity in gefitinib-treated animals. The activity of MMP2 was shown here as an internal control. The amounts of pro (a) and mature (b) MMP9 in gefitinib group decreased to 30% and 47% of that in vehicle group as measured by densitometric analysis. (E) Polarized light microscopy of unstained tibial paraffin sections from vehicle and gefitinib-treated rats. The sections were oriented with maximum birefringency (white blue). COJ is depicted as a dashed line separating growth plate (GP) and primary spongiosa (PS) areas. The intensity of birefringency was then analyzed and quantified by ImageJ. n=6/group. b: $p<0.01$ vs. vehicle. (F) Immunostaining of type II collagen in the growth plate. (G) Immunostaining of collagenase-produced 3/4 cleavage fragment of type II collagen. (H) Western blot of protein lysates from growth plate tissues using an antibody to the MMP-cleaved aggrecan product.

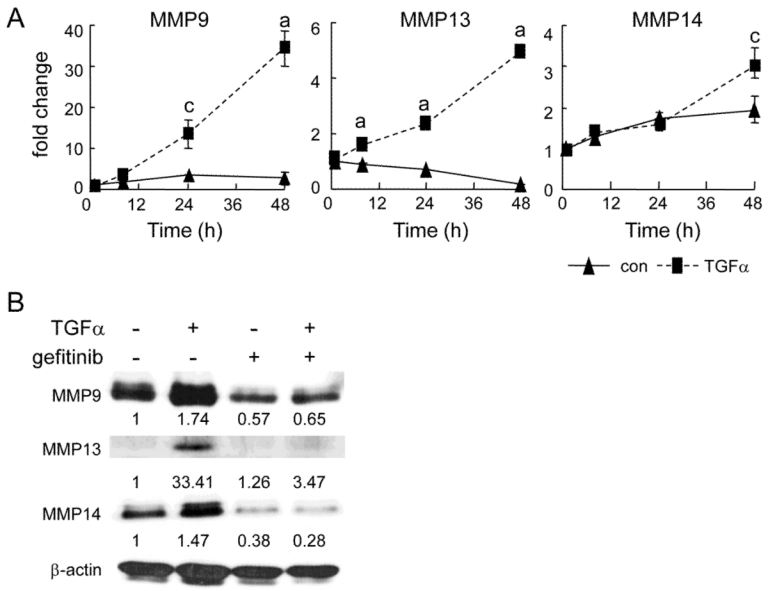

Figure 6. EGFR signaling regulates MMP9, 13 and 14 expression in primary chondrocytes

(A) Time course of TGFα regulation of MMP expression. The mRNA levels were analyzed by qRT-PCR and adjusted to the mRNA level in the control harvested at 1 h. a: $p<0.001$; c: $p<0.05$ vs. control. (B) Western blots of MMP proteins in the primary chondrocytes after 4 days of TGFα treatment. Medium was changed after 2 days along with the addition of fresh TGFα. In the gefitinib lanes, 5 μM gefitinib was added to the cells 1 h prior to TGFα treatment. The blots were quantified by densitometric measurement. The data were normalized against β-actin and the corresponding values were shown underneath each blot.

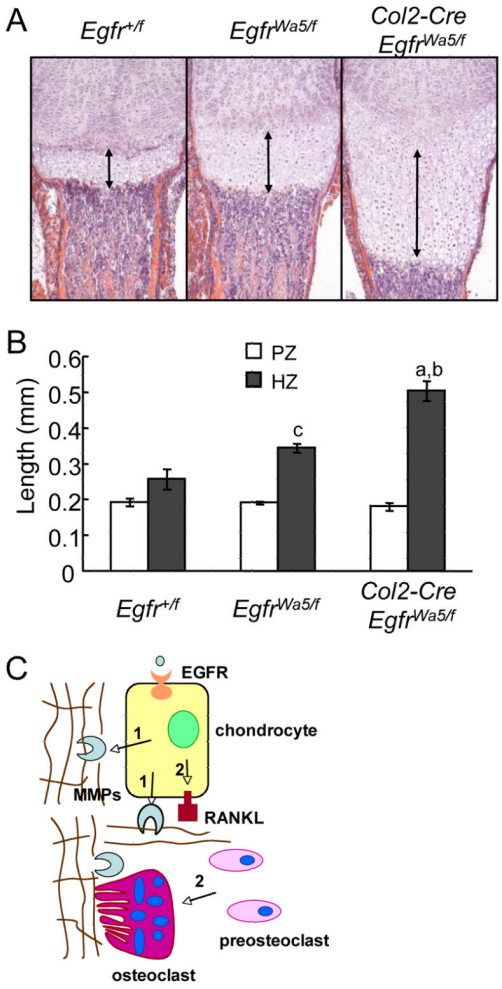

Figure 7. Mice deficient in chondrogenic EGFR activity exhibit enlarged hypertrophic zone

(A) H&E staining of tibial growth plate from *Col2-Cre* $Egfr^{Wa5/f}$ mice and controls. Double arrow lines indicate the hypertrophic zone. (B) Quantification of the lengths of proliferative (PZ) and hypertrophic (HZ) zones. n=4-5/group. a: $p<0.001$ vs $Egfr^{+/f}$; b: $p<0.005$ vs $Egfr^{Wa5/f}$; c: $p<0.05$ vs $Egfr^{+/f}$. (C) A model of how EGFR signaling stimulates cartilage degradation. Two mechanisms contribute to this function of EGFR. First (1), EGFR signaling up-regulates the expression of MMPs (9, 13, and 14) in the growth plate and thus is responsible for cartilage ECM degradation. Second (2), EGFR signaling is important for RANKL expression in the growth plate and thus is responsible for osteoclastogenesis at the COJ.